# Atrophy measurement based on segmentation propagation and the boundary shift integral technique

Marc Modat[1], Kelvin K. Leung[2], M. Jorge Cardoso[1], Nick C. Fox[2]

[1] Centre for Medical Imaging Computing, Department of Medical Physics and Bioengineering, University College London, UK,
[2] Dementia Research Centre, Institute of Neurology, WC1N 3BG, University College London, UK.

**Abstract.** Using segmentation propagation, label fusion and the boundary shift integral method, we analysed the data provided for the MICCAI'12 challenge entitled: "Atrophy measurement biomarkers using structural MRI for Alzheimers disease: a challenge to assess measurement reliability and bias". The fully automated pipeline we used, based on open-source software, is detailed in this paper along with some of the result.

## 1 Introduction

Alzheimer's disease (AD) is the main neurodegenerative disease and the prevalence of the disease is expected to raise as the overall population ages. Even though the cascade of events leading to AD largely remains unknown, the symptoms of the disease have been well studied. One can for example use the brain tissue atrophy to separate, with some accuracy, healthy subjects form patients diagnosed with AD. Brain atrophy can also be use to track changes when multiple scans from a single patient have been acquired over time. Whereas the total brain volume of an healthy elderly subject is expected to decrease by approximatively 0.5 % per year, the total brain volume of a patient diagnosed with AD decrease by approximatively 2.5 %. Hippocampal atrophy or ventricles expansion are more pronounced biomarkers which enable early detection of the atrophy process in the brain.

Reliable and accurate tools are required to quantify these volume changes as they are used to track the disease progression and help early detection of patients with neurodegenerative conditions. Indeed, although there is no cure for AD, drugs that act on the symptoms of the disease are available and an early detection of the patient is crucial. Early intervention could for example be effective in improving cognitive function, treating depression, improving caregiver mood and delaying institutionalisation[3]. The reliable and accurate monitoring of disease progression is also crucial for clinical trials and natural history studies.

[3] `http://www.alz.co.uk/research/WorldAlzheimerReport2011.pdf`

In order to quantify total brain or region-specific volume changes, the first task is to identify the relevant area. Several methods have been proposed in the literature to segment the brain tissues from non-brain tissues or fluid [1–3] or to segment specific regions of interest [4, 5]. Several techniques have also been proposed in order to quantify over time volume change in specific regions of interest (ROIs) [6, 7].

We propose to use a pipeline based on segmentation propagation and label fusion to identity three main ROIs: full brain, ventricles and hippocampi. The boundary shift integral (BSI) technique is then used to quantify ROI volume change between each pair of scan available. This pipeline is described in the next section. The following section presents some of our results before we lastly discuss these results.

## 2 Method

### 2.1 Preprocessing

The first preprocessing step we applied to all images provided for the challenge was intensity non-uniformity correction. Figure 1 shows one input image before and after intensity non-uniformity correction. In order to correct for bias field, we used the N3 algorithm [8, 9].

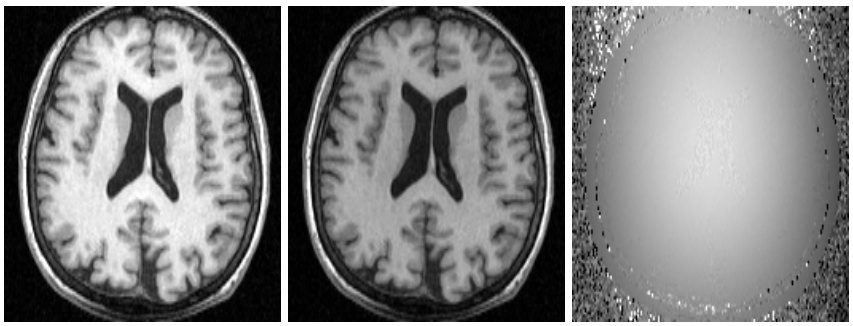

**Fig. 1.** Intensity non-uniformity correction. An axial view of scan 248_F is shown before (left-hand side) and after (middle) correction. The recovered bias field is shown in the right-hand side image.

The second preprocessing step consisted of performing a groupwise affine registration between all images: the provided images for the challenge and the images from our template library. All registrations performed to create the groupwise space were run using a block-matching approach [10]. All obtained transformations were used to update the header information of each individual image. Note that since we updated the header information was updated, no resampling of the input images has been performed. As a result, all images were then affinity

registered in physical space removing the need for any pairwise affine registration in the segmentation propagation stage.

### 2.2 Segmentation propagation and label fusion

We use a two-step process (segmentation propagation and label fusion) for the segmentations of the brain, hippocampus and lateral ventricles. We define 'query image' as the image to be segmented and 'template images' as a set of structural images with associated manual segmentations. In order to segment the ROIs, several template images are first registered to the query image and secondly all propagated segmentations are fused into a consensus segmentation.

**Non-rigid image registration** All non-rigid registrations between template library images and query images were performed using a cubic B-Spline parametrisation algorithm [11].

Briefly a grid of regularly-spaced control points is overlaid on a query image. The positions of the control point are used to parametrise a continuous deformation field which enables the warping of a template image into the space of a query image. The similarity between a query image and a deformed template image is assessed using the normalised mutual information (NMI), a measure based on the theory of entropy.

Maximising the NMI corresponds to maximising the amount of information that one image shares about the other and vice-versa. In order to promote the smoothness of the transformation and to ensure its one-to-one mapping property, a bending energy penalty term and a Jacobian determinant based penalty term are added to NMI. The positions of the control point are then optimised until maximisation of the overall objective function: the NMI plus both penalty terms. We used the implementation of the NiftyReg package [12] available from `http://sourceforge.net/projects/niftyreg`.

All obtained non-rigid transformations were then used to warp the segmentations associated with every images from the template library to the space of the query images.

**Label fusion** In order to obtain a consensus segmentation from all propagated segmentations, we used the similarity and truth estimation for propagated segmentations (STEPS) algorithm. This method uses a probabilistic formulation of the label fusion problem where the likelihood of the complete data is maximised given the set of row normalised confusion matrices [13].

In a segmentation propagation and label fusion setting, not all the propagated labels provide beneficial information due to registration errors and variability between subject's morphometries. Thus, by curating and selecting the best local labels to use, one can increase the performance of the fusion algorithm. The STEPS approach only fuses the locally best ranked deformed templates according to the locally normalised cross correlation (LNCC) between the registered template images and the query image.

Finally, in order to remove the bias introduced in the parameter optimisation due to different sizes, STEPS assumes that if all the classifiers agree on a label at a certain spatial position, then the voxel is marked as solved and is not taken into account from the estimation of the confusion matrix. A Markov random field (MRF) is also added to act as a denoiser algorithm.

Overall, the fusion method we used can be described as a combination of an LNCC ranking, an MRF and two STAPLE modifications regarding both the introduction of the local indicator function and the removal of consensus voxels from the parameter estimation. We refer the reader to Cardoso *et al.* [14] for more details about the method and implementation `http://sourceforge.net/projects/niftyseg`.

### 2.3 Longitudinal volume change assessment

Once all query images have been automatically segmented, we use the boundary shift integral (BSI) approach to quantify ROI-based volume change. The BSI involved two pre-processing steps: registration and differential bias correction.

**Intra-subject image registration** We used a symmetric registration scheme to perform the affine registration of all the time-points of the same subject, in order to avoid any systematic bias introduced by the registration process [3]. This first involved the pairwise affine registrations of all the time-points of the same subject. A middle position was given by the log-Euclidean average of all the pairwise transformations. All the time-points were then transformed to this middle position.

**Differential bias correction** A symmetric differential bias correction (DBC) scheme was used to correct for the different intensity bias between the intra-subject scans. Similar to the symmetric registration scheme, we first calculated the pairwise differential bias field of all the time points [15, 3]. A middle bias field was found by calculating the geometric mean of all the pairwise differential bias fields. All the time-points were corrected such that they had the same middle bias field. Note that for all images we already performed an intensity non-uniformity correction and the DBC addressed the residual bias field.

**Boundary shift integral** The BSI is an automated measure of regional and global cerebral atrophy rates from serial MRI which uses intra-subject image registration to give higher precision than is typically possible with manual measures [6]. The BSI estimates the changes in cerebral volume using differences in voxel intensities between two serial MRI volume scans at the boundary region of the brain. A recent improvement of BSI includes the use of tissue-specific intensity normalisation and automatic parametric selection [16] that improve the robustness and reproducibility of BSI. Furthermore, for the hippocampal BSI, a double intensity window approach was used to capture boundary shift

at both the hippocampus  cerebrospinal fluid border, and the hippocampus  white matter border [17]. The source code for BSI can be downloaded from `http://sourceforge.net/projects/bsintegral`.

### 2.4 Template library

The template library we used here consisted of 89 T1-weighted MR images. For each image in the template library, we had associated manual segmentations of the brain and the ventricles. We also had manual segmentations of the left and right hippocampi for 66 images from the template library.

All images from the template library were flipped along the left-right axis resulting in 178 T1-weighted MR image, with 178 associated brain and ventricles segmentations and 132 hippocamppi segmentations.

We must emphasise that although we have previously used the test dataset provided for the atrophy challenge in a template library, the template library in this work does not contain any images and segmentations from the test dataset.

## 3 Dataset for the atrophy challenage

The dataset provided for the challenge consisted of T1-weighted MRI scans of 69 subjects: 46 diagnosed with AD and 23 age-matched elderly controls. All subjects have been scanned at 0, 2, 6, 12, 26, 38 and 52 weeks and a subset has also been scanned at 18 and 24 months. The data acquisition was performed on a 1.5 T Signa Unit (GE Medical Systems, Milwaukee) with a inversion recovery (IR)-prepared spoiled GRASS sequence: TE 6.4 ms, TI 650 ms, TR 3000 ms, bandwidth 16 kHz, $256 \times 256 \times 128$ matrix with a field of view of $240 \times 240 \times 186$ mm.

## 4 Implementation details and parameters used

In order to segment each of the 708 T1-weighted MR images provided we performed $708 \times 178$ (126,024) non-rigid registrations. For each registration, the control point spacing was set to 2.5 voxel along each axis. The weight of the bending energy and Jacobian-based penalty terms were set to 1% and 0.5% of the overall objective function respectively. A coarse-to-fine approach was used using 4 levels and the maximal number of iteration per level was set to 1000.

For each fusion of the propagated segmentations, the LNCC was computed using a Gaussian kernel with a standard deviation of 2 millimetres and only the 15 local best propagations were considered to extract a consensus.

The intra-subject global registration were performed over the brain mask subject dilated by 10 voxels. The normalised cross correlation was used as a measure of similarity. All subject images were resampled to a groupwise space using a windowed sinc interpolation scheme with a Welch window of radius 5. A 5-voxel radius median filter was used to compute the differential bias correction. The BSI regions were computed using a dilation and an erosion of 1 voxel

respectively and the tissue intensity estimation using k-means clustering was performed using a 3 voxels dilation.

## 5 Result

Figure 2 shows the volume of the different ROIs for each subject. Note that these volumes were not used to quantify volume changes but only used to initialise the BSI technique.

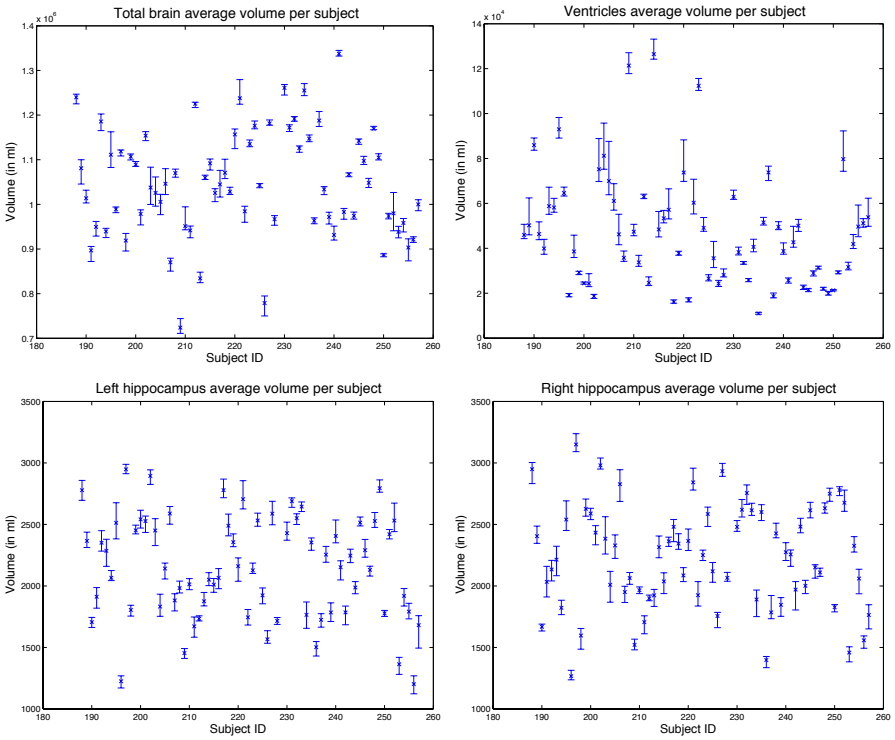


**Fig. 2.** Average volume per subject for each ROI. The error bars correspond to the minimal and maximal volumes for each subject and ROI.

Figure 3 presents for every subject the full brain BSI results. For each subject, only the differences from the baseline image are presented. Figure 4 shows coronal views of the scan 217_A and 217_G that lead to an unexpected 27.2 millilitres brain volume increase.

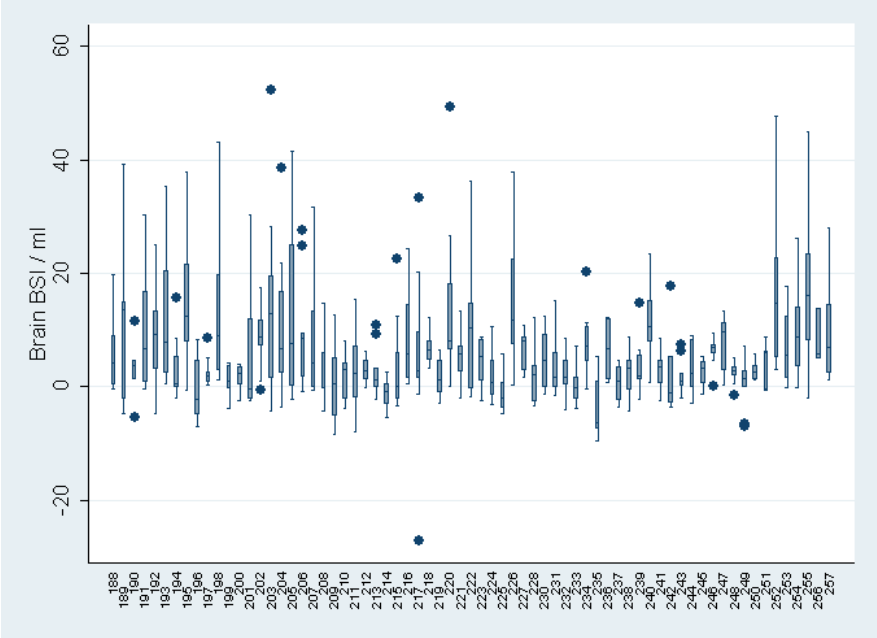


**Fig. 3.** Brain boundary shift integral result. All atrophy rates are based on comparison to the subject baseline.

## 6 Conclusion

We presented here an automated pipeline for longitudinal volume change assessment. The pipeline takes advantage of existing techniques and open-source software for registration, label fusion and BSI evaluation. The proposed framework did not include any quality check. Some result might thus be inadequate for other applications such as clinical trials due to some poor image quality, artefact or others. In a clinical trial context, all results including registration, segmentation and BSI output would be checked and manually edited if required or excluded from the study.

Details about the result will be presented during the "Atrophy measurement biomarkers using structural MRI for Alzheimers disease: a challenge to assess measurement reliability and bias" workshop and MICCAI'12 in Nice, France.

## Acknowlegment

The authors would like to thank Tristan Clark for his support with the UCL Computer Science computer cluster.

Marc Modat was supported by CBRC grant 168. Jorge M. Cardoso was funded by Fundacao para a Ciencia e a Tecnologia, Portugal. Kelvin K. Leung received some founding from ADNI. Nick C. Fox was employed by University

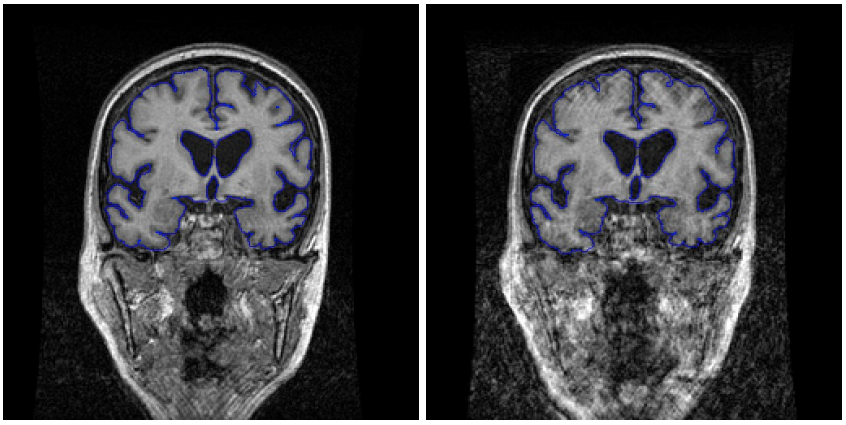

**Fig. 4.** Coronal view of the scans 217_A (left-hand side) and 217_G (right-hand side). The automatic brain segmentation is outlined in blue. Note the motion artefact that lead to a wrong brain atrophy estimation using the BSI technique.

College London Hospitals/University College London, which received a proportion of funding from the Department of Health's National Institute for Health Research Biomedical Research Centres funding scheme. The Dementia Research Centre is an Alzheimer's Research Trust Coordinating Centre and has also received equipment funded by the Alzheimer's Research Trust. Nick C. Fox is a MRC Senior Clinical Fellow and National Institute for Health Research Senior Fellow.

## References

1. Smith, S.M.: Fast robust automated brain extraction. Hum. Brain Mapp. **17**(3) (Nov 2002) 143–155
2. Segonne, F., Dale, A., Busa, E., Glessner, M., Salat, D., Hahn, H., Fischl, B.: A hybrid approach to the skull stripping problem in MRI. Neuroimage **22**(3) (Jul 2004) 1060–1075
3. Leung, K.K., Barnes, J., Modat, M., Ridgway, G.R., Bartlett, J.W., Fox, N.C., Ourselin, S., ADNI Study: Brain MAPS: an automated, accurate and robust brain extraction technique using a template library. NeuroImage **55**(3) (Apr 2011) 1091–1108
4. Fischl, B., van der Kouwe, A., Destrieux, C., Halgren, E., Segonne, F., Salat, D., Busa, E., Seidman, L., Goldstein, J., Kennedy, D., Caviness, V., Makris, N., Rosen, B., Dale, A.: Automatically parcellating the human cerebral cortex. Cereb. Cortex **14**(1) (Jan 2004) 11–22
5. Heckemann, R.A., Hajnal, J.V., Aljabar, P., Rueckert, D., Hammers, A.: Automatic anatomical brain MRI segmentation combining label propagation and decision fusion. NeuroImage **33**(1) (Oct 2006) 115–126
6. Freeborough, P.A., Fox, N.C.: The boundary shift integral: an accurate and robust measure of cerebral volume changes from registered repeat MRI. IEEE Transactions on Medical Imaging **16**(5) (Oct 1997) 623–629

7. Smith, S.M., Zhang, Y., Jenkinson, M., Chen, J., Matthews, P.M., Federico, A., De Stefano, N.: Accurate, robust, and automated longitudinal and cross-sectional brain change analysis. NeuroImage **17**(1) (Sep 2002) 479–489
8. Sled, J., Zijdenbos, A., Evans, A.: A nonparametric method for automatic correction of intensity nonuniformity in MRI data. IEEE Transactions on Medical Imaging **17**(1) (Feb 1998) 87–97
9. Boyes, R.G., Gunter, J.L., Frost, C., Janke, A.L., Yeatman, T., Hill, D.L.G., Bernstein, M.A., Thompson, P.M., Weiner, M.W., Schuff, N., Alexander, G.E., Killiany, R.J., DeCarli, C., Jack, C.R., Fox, N.C., ADNI Study: Intensity non-uniformity correction using N3 on 3-T scanners with multichannel phased array coils. NeuroImage **39**(4) (Feb 2008) 1752–1762
10. Ourselin, S., Roche, A., Subsol, G., Pennec, X., Ayache, N.: Reconstructing a 3D structure from serial histological sections. Image and Vision Computing **19**(1-2) (Jan 2001) 25–31
11. Rueckert, D., Sonoda, L., Hayes, C., Hill, D., Leach, M., Hawkes, D.: Nonrigid registration using free-form deformations: Application to breast MR images. IEEE Transactions on Medical Imaging **18**(8) (Aug 1999) 712–721
12. Modat, M., Ridgway, G.R., Taylor, Z.A., Lehmann, M., Barnes, J., Hawkes, D.J., Fox, N.C., Ourselin, S.: Fast free-form deformation using graphics processing units. Comput Meth Prog Bio **98**(3) (Jun 2010) 278–84
13. Warfield, S.K., Zou, K.H., Wells III, W.M.: Simultaneous truth and performance level estimation (STAPLE): an algorithm for the validation of image segmentation. IEEE Transactions on Medical Imaging **23**(7) (Jul 2004) 903–921
14. Cardoso, M.J., Modat, M., Keihaninejad, S., Cash, D., Ourselin, S.: Multi-STEPS: Multi-label similarity and truth estimation for propagated segmentations. In: Mathematical Methods in Biomedical Image Analysis (MMBIA), 2012 IEEE Workshop on. (2012) 153–158
15. Lewis, E.B., Fox, N.C.: Correction of differential intensity inhomogeneity in longitudinal MR images. Neuroimage **23**(1) (Sep 2004) 75–83
16. Leung, K.K., Clarkson, M.J., Bartlett, J.W., Clegg, S., Jack, C.R., Weiner, M.W., Fox, N.C., Ourselin, S., ADNI Study: Robust atrophy rate measurement in Alzheimer's disease using multi-site serial MRI: tissue-specific intensity normalization and parameter selection. NeuroImage **50**(2) (Apr 2010) 516–523
17. Leung, K.K., Barnes, J., Ridgway, G.R., Bartlett, J.W., Clarkson, M.J., Macdonald, K., Schuff, N., Fox, N.C., Ourselin, S., ADNI Study: Automated cross-sectional and longitudinal hippocampal volume measurement in mild cognitive impairment and Alzheimer's disease. NeuroImage **51**(4) (Jul 2010) 1345–1359